Supplements:

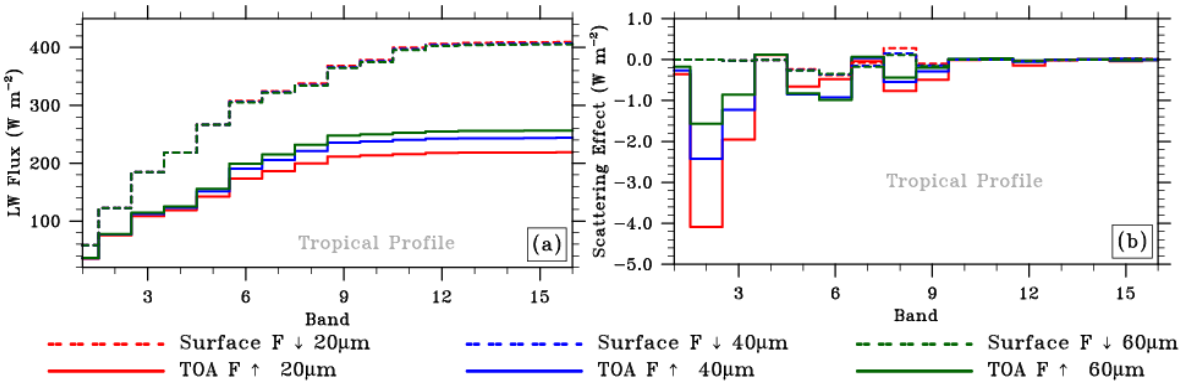

Figure S1. Cumulative band-by-band downward LW fluxes at surface (dash lines) and upward LW fluxes at TOA (solid lines) from RRTMG_LW with the original LW radiation calculation (left column) and the difference caused by the LW scattering effect in each band (right column). The red, blue and green lines represent the respective results with D_{ge} equal to 20, 40, and 60μm of the high ice cloud case prescribed in the given tropical profile.

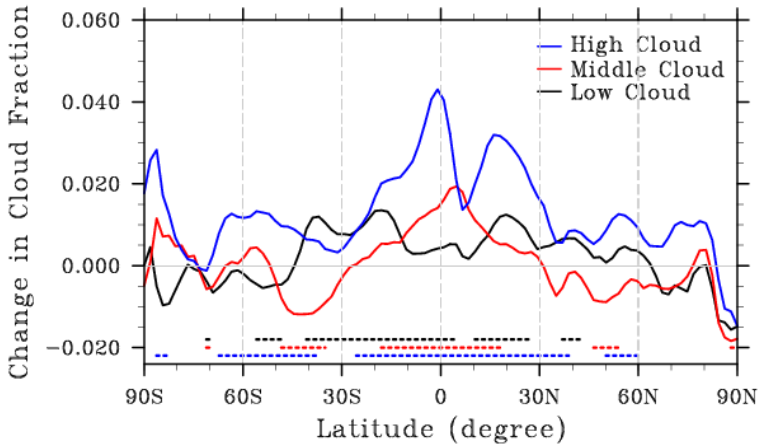

Figure S2. Interactive runs: cloud LW scattering effect on annual zonal averaged cloud fractions at low (black curves), middle (red curves), and high (blue curves) levels. (The dashed lines underneath mark the significances for each variable at the 90% confidence level using the Student's *t* test).

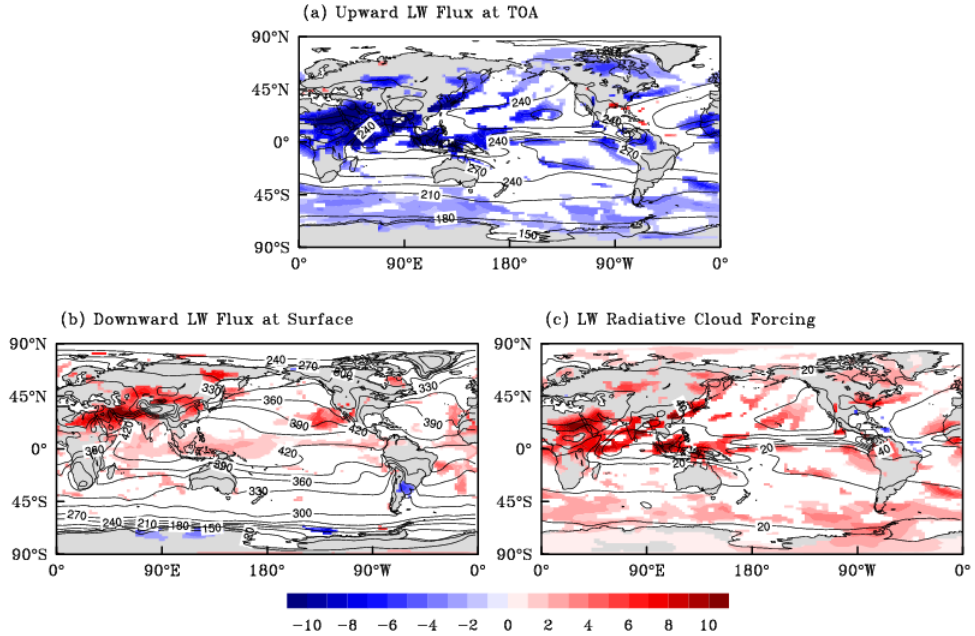

Figure S3. Interactive runs: the color contours show the cloud LW scattering effect on semiannual (monsoon period during warm seasons from April to September) gobal distributions of upward LW flux at TOA (**a**), downward LW flux at surface (**b**), and LW cloud forcing at TOA (**c**). Results from reference run with the origianl RRTMG_LW are plotted as solid contour lines. (Results shown with colors are significant at the 90% confidence level using the Student's *t* test).

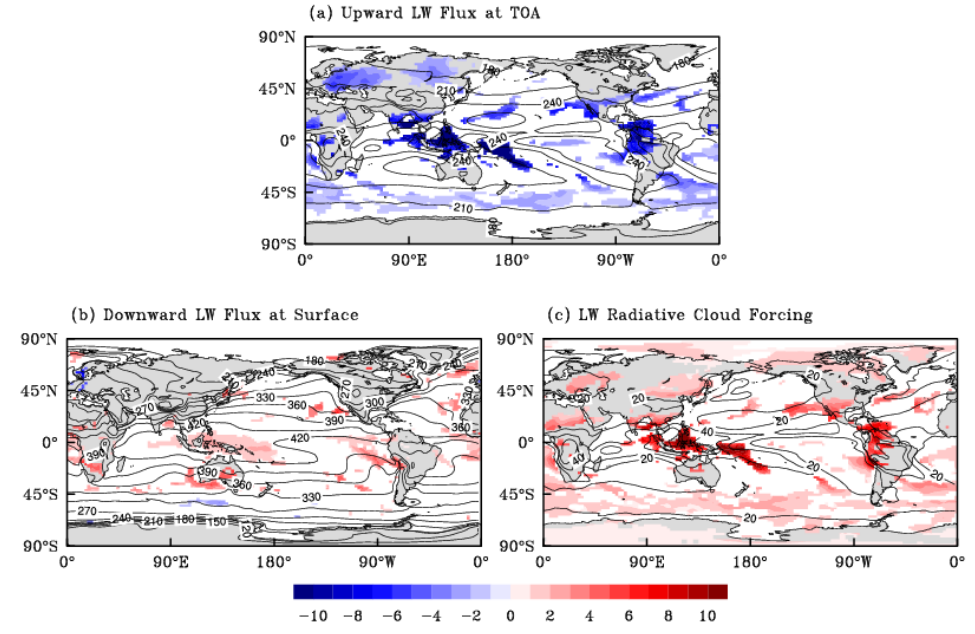

Figure S4. The same as Figure S3, but for the cold seasons from October to March.

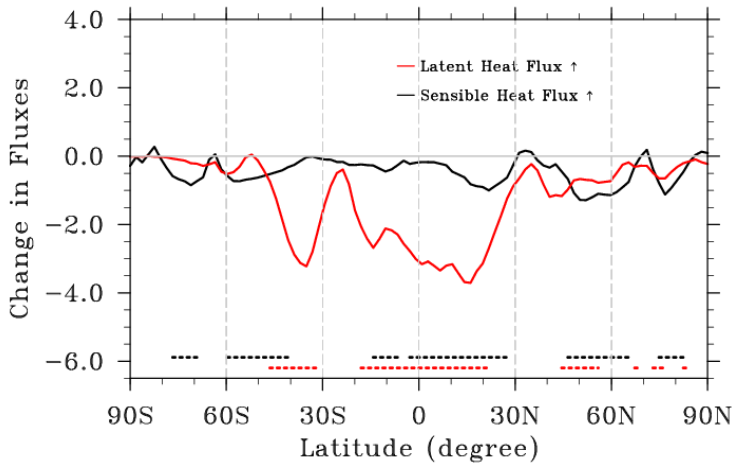

Figure S5. Interactive runs: cloud LW scattering effect on annual zonal averaged sensible heat flux (black curves) and latent heat flux (red curves). (The dashed lines underneath mark the significances for each variable at the 90% confidence level using the Student's *t* test).

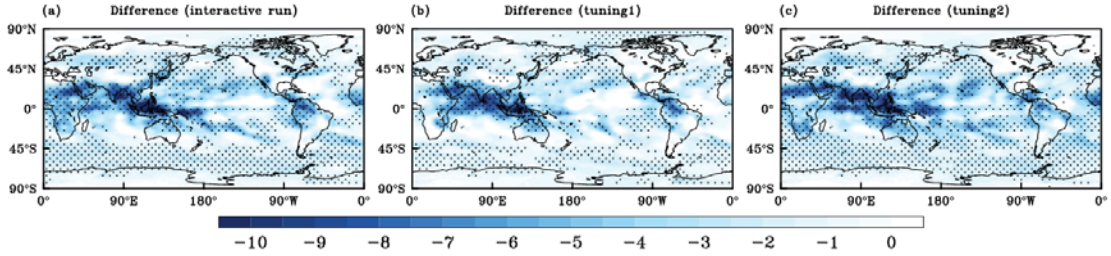

Figure S6. Cloud LW scattering effect on the annual global distributions of upward LW flux at TOA (i.e. differences between the interactive run (a)/tuning 1 (b)/tuning 2 (c) and the reference run; Dotted regions are significant at the 90% confidence level using the Student's *t* test; Figures in units: W m^{-2}).

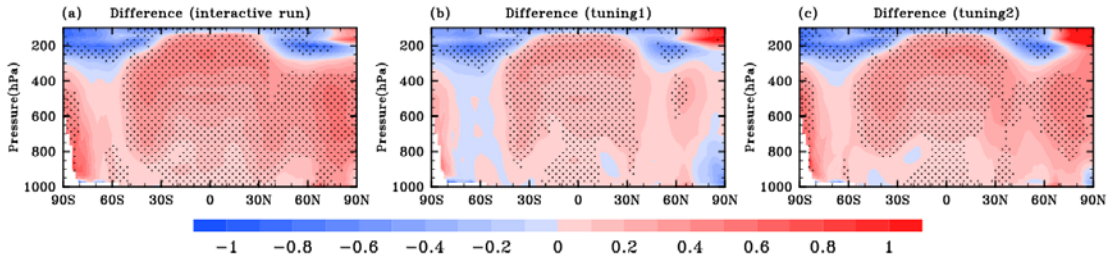

Figure S7. Cloud LW scattering effect on annual zonal mean of temperature (i.e. differences between the interactive run (a)/tuning 1 (b)/tuning 2 (c) and the reference run; Dotted regions are significant at the 90% confidence level using the Student's *t* test; Figures in units: K).

Table S1. Annual global mean radiative fluxes/forcing (W m^{-2}) in CAM5 runs. CERES (Clouds and the Earth's Radiant Energy System) data refer to Bacmeister et al. [65]. TOM: top of model; SWCF: shortwave cloud forcing; LWCF: LW cloud forcing.

		CAM5	CAM5+DISORT_8S		
Energy flux/Forcing	**CERES**	**Reference**	**Interactive**	**Tuning1**	**Tuning2**
Residual (TOM)	−	2.5	3.9	2.5	2.5
Net longwave (TOM)	−	233.1	230.7	231.3	230.1
Net shortwave (TOM)	−	235.5	234.7	233.8	232.6
LWCF	26.5	24.7	26.6	25.6	26.9
SWCF	-47.1	-52.4	-53.3	-54.1	-55.6
Clear-sky longwave (TOA)	266.5	259.1	258.7	258.4	258.4
Clear-sky shortwave (TOA)	287.6	291.3	291.4	291.3	291.7

In Section 4.2, the net energy flux at the top of the model (TOM) has imbalance in the interactive run. Here we conduct two "tuning" on the interactive run so that the residual energy at TOM becomes same as the reference run. The tuning 1 run changes the cloud microphysical property. The autoconversion threshold for cloud ice to snow is tuned from 400 to 330 to reduce the ice cloud water path. The tuning 2 run changes the cloud macrophysical property. The relative humidity threshold for low cloud fraction is changed from 0.8975 to 0.8675 to increase the low cloud fraction. The LW cloud scattering effects on the upward flux at TOA and on temperature are plotted in Figure S6 and Figure S7 for tuning 1 and tuning 2 runs.